PRAMANA
— journal of
physics

Vol. 40, No. 4,
April 1993
pp. 311–320

Collective dipole oscillations in atomic nuclei and small metal particles

R S BHALERAO and MUSTANSIR BARMA
Theoretical Physics Group, Tata Institute of Fundamental Research, Homi Bhabha Road, Bombay 400 005, India
Email: Bhalerao @ tifrvax.bitnet; Barma @ tifrvax.bitnet

MS received 3 December 1992

Abstract. The systematics of photon absorption cross sections in nuclei and small metal particles are examined as a function of the number of constituent fermions A. It is pointed out that the shell-structure-linked oscillations in the full width at half maximum (FWHM) of the photoneutron cross section in nuclei, earlier recognized for $A > 63$, in fact persist down to the lightest nuclei. Averaging over the oscillations or focusing on the lower envelope of the oscillating curve (magic nuclei), the FWHM is seen to generally decrease with increasing A, consistent with $A^{-1/3}$, a dependence which was earlier known to hold in metal particle systems. If the FWHMs are scaled by the respective Fermi energies and the inverse radii by the Fermi wave vectors, the two data sets become comparable in magnitude. A schematic theoretical description of the systematics is presented.

Keywords. Giant dipole resonance; Mie resonance; small metal particles; metal clusters; shell effects; size dependence.

PACS Nos 24·30; 25·20; 36·40; 78·40

1. Introduction

It is becoming increasingly clear that there are certain points of strong resemblance between the electronic properties of metal particles or clusters, and the properties of atomic nuclei [1]. Electrons in metal particles and nucleons in nuclei both constitute finite Fermi systems with temperatures much less than the respective Fermi energies—a fact which cuts across the very different scales of length, mass and energy in the two systems. Metal particles, like nuclei (and unlike atoms), exhibit saturation, or constancy of particle density, with increasing size. Also, shell structure in energy levels —long familiar in nuclear physics—manifests itself in the relative abundances, polarizabilities and ionization potentials of metal particles as well [2].

Here we focus on another aspect of the analogy, namely, the response of metal particles and nuclei to electromagnetic radiation. In both systems, the field resonantly excites a collective dipolar mode, and the wavelength of the radiation at resonance far exceeds the size of the system. In nuclei, it is the giant dipole resonance (GDR), in which protons are displaced with respect to neutrons and strong interactions provide the restoring force (see, e.g. [3, 4]). In metal particles, the Mie resonance involves displacing the conduction electron cloud with respect to the background of positive ions, and there are electromagnetic restoring forces (see, [5–7]). In this paper, we explore the systematics of these two sets of data with varying numbers of fermions.

In § 2, we discuss the available data for both nuclei and metal particles, and draw

some empirical conclusions regarding systematic trends, with an emphasis on the FWHMs. This is our main result. In § 3, we present a schematic theoretical description for the size dependence of the width. A brief account of this work has already appeared [8].

2. Cross-section systematics

2.1 *Nuclei*

Photo-neutron cross-sections have been measured in a large number of nuclei, and plots of the measured cross sections as a function of incident photon energy, $\sigma(E)$, have been compiled by Dietrich and Berman [9]. For spherical nuclei, the cross section for the photoexcitation of GDR has a single maximum, while for deformed nuclei there is more than one maximum (see, [3]). In the former case, the peak frequency ω_0 is known to exhibit a systematic empirical dependence on the mass number A:

$$\omega_0 = 31{\cdot}2A^{-1/3} + 20{\cdot}6A^{-1/6}\text{MeV}. \tag{1}$$

We shall discuss this dependence (vis-à-vis the A independence of ω_0 in metal particles) in § 3·1. The FWHM provides a simple, single characterization of the resonance spectrum, and has been used earlier to extract global trends with varying A, for heavier nuclei. For instance, Bergére [10] and Snover [11] have shown plots of the FWHM in the regions $A > 90$ and $166 > A > 63$, respectively. These plots show that the FWHM exhibits systematic oscillations in the ranges studied, with local minima near spherical, near-magic nuclei.

Instead of FWHM, an alternative characterization of the data is to fit one or two Lorentzians to $\sigma(E)$, and thus extract the values of the resonance energies ω_{01} and ω_{02}, the widths Γ_1 and Γ_2, and cross sections σ_1 and σ_2, for the lower and higher energy resonances respectively. This procedure is usually applied to $A > 50$, and the values of Γ_1 and Γ_2 are given by Dietrich and Berman [9]. We have observed that if the width corresponding to the larger cross section is plotted versus A, then the result shows trends similar to those exhibited by the FWHM. However, the FWHM has the added advantage that it can be used across the periodic table.

We wanted to see whether the systematics observed earlier for the FWHM of heavier nuclei [10, 11] persisted in lighter nuclei as well. We examined the FWHM in about 120 nuclei ranging from ^{3}He to ^{239}Pu, using primarily the cross-section data compiled by Dietrich and Berman [9]. (We re-examined the heavier nuclei in order to have a uniform procedure for all A.) For those cases where the data follow a curve with a single peak, it was straightforward to determine the FWHM. For cases with two or more (closely overlapping) peaks, we found the FWHM by drawing a smooth curve with a single maximum through the data points, trying to ensure that the areas under the smooth curve and the experimental data were nearly equal. Those nuclei where the data seem incomplete (^{3}H, ^{19}F) or have too much structure (^{14}C, ^{18}O, ^{24,26}Mg) were ignored. Results are displayed in figure 1. For light nuclei (see inset in figure 1), we also estimated the errors in the FWHMs, arising from (a) the existence of more than one data set in some cases, and (b) the inherent uncertainty in extracting the FWHM by our procedure. In the range $A > 90$, our values agree well with those of Bergére [10]. A determination of the FWHM using least-square fits to a smooth single-peaked curve would be more rigorous, but we do not expect it to change our estimated values enough to affect our conclusions.

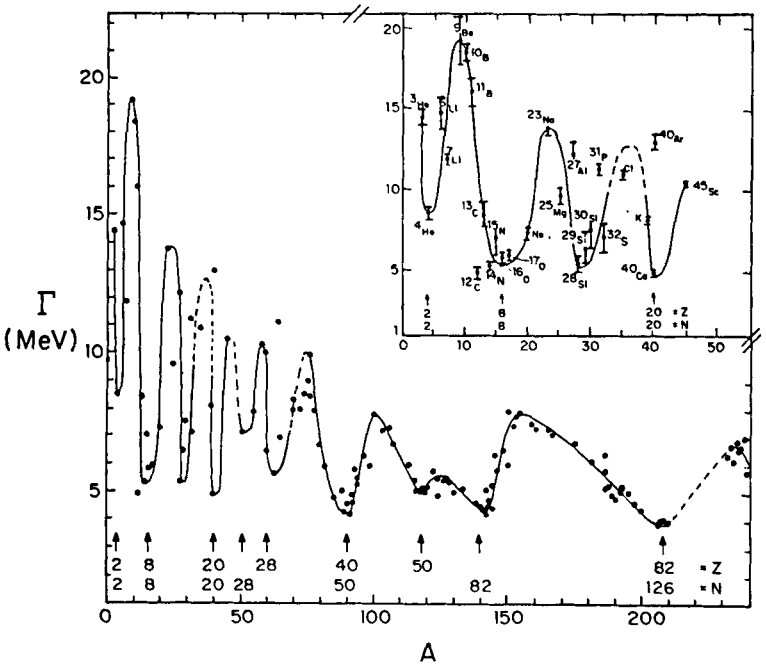

Figure 1. Γ is the full width at half maximum of the total photoneutron cross section on a nucleus when plotted as a function of the incident photon energy. Compilation of the cross-section data by Dietrich and Berman [9] was used to determine Γ. Note the systematic modulations in the Γ vs A curve, with minima at the proton (Z) or neutron (N) magic numbers. The minimum at $A = 28$ corresponds to ^{28}Si, see [12]. The curve is drawn as a guide to the eye. Dashed lines indicate regions of sparse or nonexistent data. The inset shows the region $A \leqslant 45$ in greater detail. (Γ for Ne, Cl and K is obtained from data on natural samples.) The statistical significance of the oscillations of the curve is discussed in the text.

Examination of the results in figure 1 for light nuclei ($A < 50$) (see the inset) shows that the FWHM continues to display local minima at, by and large, the magic numbers. The rapid oscillations of the FWHM versus A are due to the relative crowding in of magic numbers for small A. With the sole exception of ^{28}Si, all the minima occur at or near the magic numbers [12]. Conversely, each magic number has a corresponding minimum, with the possible exception of $N = 40$ ($A = 72$), where there is a hint of a local minimum, but the data do not allow us to draw a firm conclusion. In any case, 40 is known to be a weak magic number.

The systematic oscillations in the region $A < 50$ in figure 1 are statistically significant. As is evident from the inset, the error in the FWHM is less than 1 MeV in almost all cases, and is generally much smaller. The amplitude of oscillations, on the other hand, is at least 5–6 MeV (e.g., ^{3}He to ^{4}He, or ^{40}Ca to ^{45}Sc), and is sometimes as large as 14 MeV (e.g., ^{9}Be to ^{14}N). The oscillations are as systematic and as pronounced as those for large A, the only difference being that there are fewer points per oscillation.

That the photo-response of a nucleus even as light as He can be thought of in the same terms as that of heavier nuclei may seem suprising, but the very fact that the widths for light nuclei fit in well with the systematics across the periodic table provides an a posteriori justification for the use of the FWHM even for $A < 50$.

An interesting feature of figure 1 is the overall downward trend of the oscillatory

curve, evident if, for instance, we focus on points in the lower envelope of the curve. These points correspond mostly to spherical, magic nuclei. The manner in which the width decreases as a function of size is discussed below, in connection with figure 2.

2.2 *Metal particles*

In metal particles, the Mie resonance corresponds to the excitation of a surface plasmon. For a spherical particle, within the free electron approximation, the resonance frequency ω_0 is $\omega_p/\sqrt{3}$, where ω_p is the plasma frequency [5]. Since ω_p depends primarily only on the electron density, ω_0 does not vary very strongly with size—less than 10% as the size is decreased from ~ 100 Å to ~ 10 Å [14].

For optical absorption experiments on small metal particles, it is important to distinguish between two types of samples: (i) free metal clusters in which size separation is achieved by mass spectroscopy, and (ii) metal clusters embedded in various matrices, such as glass or solid argon. Particles are isolated from each other, but some spread in size cannot be avoided. A typical spread in radius is $\sim 20\%$.

Experiments on samples of type (i) have been performed on small metal clusters with between 2 and 40 conduction electrons [15–17]. The data indicate that, as with nuclei, there is a strong response over a relatively narrow frequency interval in the case of magic numbers, and over a much broader frequency range in cases which fall between magic numbers. In the latter case, the line shows splittings, which can be interpreted in terms of shape deformations.

A larger range of sizes (~ 10 Å to ~ 100 Å) has been investigated [14] in experiments on samples of type (ii). No noticeable oscillations in Γ versus radius R have been observed with such samples, but this is probably because (a) unlike for nuclei, oscillations are averaged out due to the distribution of sizes, and (b) the amplitude of shell-structure-linked oscillations is expected to decrease with increasing size, and thus be small for the above range of sizes. However, these experiments do reveal a systematic dependence of the averaged FWHM Γ_{av} on R:

$$\Gamma_{av} = K\frac{\hbar v_F}{R} + \Gamma_\infty, \tag{2}$$

where v_F is the Fermi velocity, K is a constant of order unity and Γ_∞ is the width in the bulk medium. Equation (2) describes the variation of the linewidth of Ag particles in a variety of host matrices. The constant K depends on the matrix [14], it goes down by a factor ~ 3 as the matrix is changed from glass to an inert element solid like Ar and Ne, presumably due to surface effects.

2.3 *Similarities and differences between nuclei and metal particles*

We wanted to see if (2), which holds for metal particles with a spread in sizes, also describes the downward trend of Γ in nuclei with increasing A, evident in figure 1. A similar $1/R$ dependence has been discussed earlier [18] for nuclei in the range $A > 50$. On dividing across by the Fermi energy ε_F, we see that (2) predicts that $\Gamma_{av}/\varepsilon_F$ is a linear function of $(k_F R)^{-1}$, where k_F is the Fermi wave vector. Interestingly, on using these dimensionless scaled variables, we can directly compare the Ag-particle and nuclear data (figure 2) which in absolute terms differ by six orders of magnitude in energy and five orders of magnitude in length. We used the values $\varepsilon_F = 38$ MeV and $k_F = 1{\cdot}36\,\text{fm}^{-1}$ for nuclei, and $\varepsilon_F = 5{\cdot}49$ eV and $k_F = 1{\cdot}20\,\text{A}^{-1}$ for Ag particles.

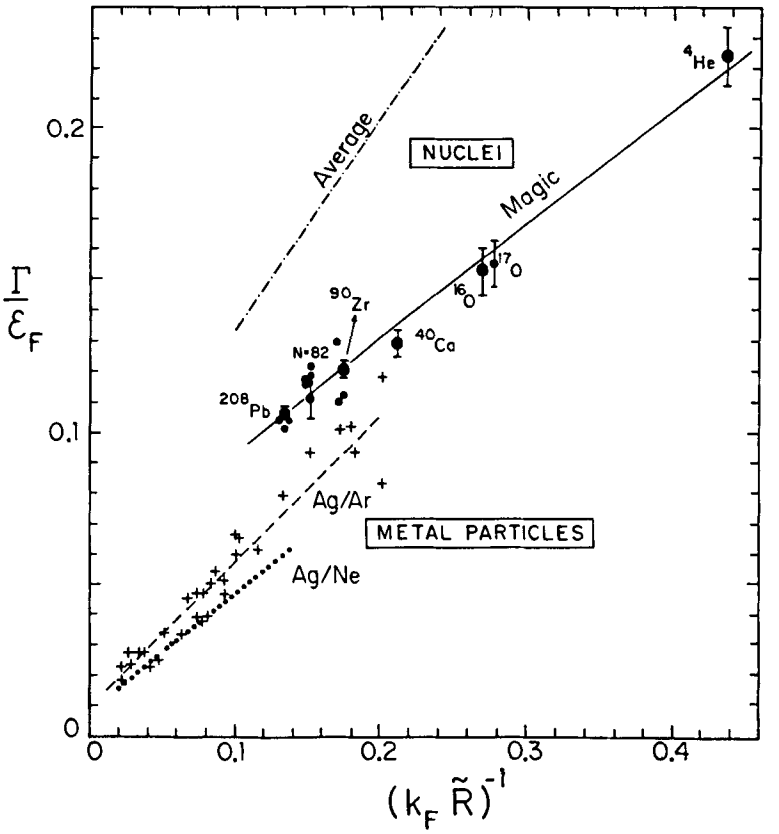

Figure 2. Γ/ε_F vs. $(k_F\tilde{R})^{-1}$ for metal particles and nuclei. Γ is the same as in figure 1. The dashed and dotted lines are best fits for Ag/Ar (+, [14, 19]) and Ag/Ne [14]. The nuclei shown here are singly (●) or doubly (●) magic nuclei from the lower envelope of the oscillating curve in figure 1. The solid straight line is the best fit to this data set. The dot-dashed line indicates the 'average' trend of the oscillatory curve in figure 1. Note the similarities between the scaled nuclear and particle data despite the fact that the two data sets differ by six orders of magnitude in energy and five orders of magnitude in length. For $A \geqslant 90$, not all error bars are shown; nuclei in the same cluster have roughly similar error bars.

We have chosen to plot data for Ag particles in argon and neon matrices as interactions with surrounding inert gas atoms are likely to be minimal, and a large range of sizes has been studied for Ag/Ar [19]. We have used RMS radii $\tilde{R}$, as these are well determined for nuclei; for Ag particles, we too $\tilde{R}$ to be given by $\sqrt{3/5}$ times the quoted radii. Since Γ oscillates as a function of size in nuclei, and we are interested in displaying the overall downward trend, we have replotted points corresponding to singly or doubly magic nuclei from the lower envelope of the curve in figure 1; the line marked 'magic' is the best fit line through these points. Thus these points are consistent with a linear dependence on $(k_F\tilde{R})^{-1}$, though other monotonic variations with $\tilde{R}$ cannot be ruled out. We also examined the average downward trend of the oscillatory curve in figure 1, and found that it could also be fit to a linear dependence. The slope of the average line (marked 'average' in figure 2) is larger than that of the solid line, and is comparable to the slopes of the dashed and dotted lines. Thus (2) holds to a good approximation for nuclei also. In particular, it is interesting to see

how well the doubly magic nuclei ^{4}He, ^{16}O, ^{40}Ca, ^{90}Zr and ^{208}Pb follow a straight line.

Of course, there are also some differences between nuclei and metal particles. We have already pointed out a difference as regards the A dependence of ω_0. The magic numbers in the two cases are also not the same for large A, because of the difference in the strengths of the spin-orbit force in the two systems. Finally, the intercepts on the Γ/ε_F axis, for the two sets of data in figure 2, are quite different. The significance of this will be discussed in the following section.

3. Discussion

In this section, we will give a schematic theoretical description of the expected systematics of the resonance with size, and see how it accords with the trends seen in experiments.

Let us begin by recalling the principal conclusions of the comparison between nuclei and metal particles. First, the resonance peak frequency ω_0 exhibits a systematic variation with A for nuclei (see (1)), whereas it is roughly size independent for metal particles. Second, the FWHM exhibits a general downward trend with increasing A, consistent with an $A^{-1/3}$ dependence (figure 2). A similar dependence is also seen in metal particle systems with a spread in sizes but with smaller intercepts on the Γ/ε_F axis. Third, the FWHM exhibits strong shell effects in nuclei, and similar tendencies in separated metal clusters. In metal particle samples with a spread in sizes, shell effects are not seen.

3.1 *Resonance frequency*

The size dependence of the natural frequency of vibration ω_0 can be deduced by using a simple classical picture of the collective mode. In the metal particle, the restoring force arises from the electric field produced by layers of opposite charges on the two sides [20] and acts on each of the A conduction electrons in the particle. The oscillator frequency ω_0 is given by the square root of the ratio of the total restoring force per unit displacement to the mass involved. Since both force and mass are proportional to A, the frequency ω_0 is roughly size independent. In the nucleus, on the other hand, the restoring force arises from short-range strong interactions amongst nucleons. In a hydrodynamic description, it is modelled by the surface or volume symmetry energy terms in the semiempirical mass formulas. In the Goldhaber–Teller model [21], the collective state corresponds to the motion of the proton cloud through the neutron cloud without mutual distortion. The restoring force is proportional to $A^{2/3}$ and the mass parameter is proportional to A. Hence, $\omega_0 \sim A^{-1/6}$. In the Steinwedel–Jensen model [22], on the other hand, the relative proton-neutron density changes in such a way as to maintain constant overall density throughout. The restoring force per unit mass is proportional to R^{-2}, and hence $\omega_0 \sim A^{-1/3}$.

3.2 *Resonance widths: overall trend*

Turning to the FWHM in nuclei, one may distinguish between two types of contributions. Firstly, there is intrinsic width of the resonance which comes from the finite lifetime of the collective mode, and which is present in all cases. The intrinsic width itself receives contributions from a variety of physical mechanisms to be discussed below. This is the only contribution to the FWHM in spherical nuclei.

Secondly, in nonspherical nuclei, static deformations in shape can lead to two distinct resonance frequencies, corresponding to a splitting of the line. In such cases, the FWHM receives additional contributions.

The intrinsic width Γ_i can be written as the sum of three terms [4]

$$\Gamma_i = \Delta\Gamma + \Gamma^{\uparrow} + \Gamma^{\downarrow}, \tag{3}$$

reflecting contributions from distinct physical effects. The fragmentation width $\Delta\Gamma$ corresponds to the fact that the collective $(1p-1h)$ state which is the doorway state for the GDR, is not a single state, but is in most cases already appreciably fragmented. This effect (mean-field damping or one-body friction) is the finite nucleus analogue of Landau damping in a bulk medium. It occurs due to the scattering of the nucleons from the 'wall' or 'surface' of the self-consistent mean field potential. The second term $\Gamma^{\uparrow}$ is the escape or decay width corresponding to the direct coupling of the $(1p-1h)$ doorway state to the continuum, giving rise to its decay into a free nucleon and an $(A-1)$ nucleus. Finally, the spreading width $\Gamma^{\downarrow}$ is due to the coupling of the $(1p-1h)$ doorway state to more complicated $(2p-2h)$ states of the nucleus, the transition occurring on account of genuine two-body effects (collisional damping or two-body friction).

Let us see how each contribution to (3) is expected to vary with radius R. Our arguments are schematic, and aimed at establishing the general, systematic trend with size.

The R-dependence of the first two terms may be estimated using a simple argument based on estimating the frequency of collisions with the surface. Such an argument has been used successfully [23] to estimate $\Delta\Gamma$ in metal particles; the estimate agrees with the result of a quantum calculation [24–26] of the fragmentation width, within a square-well model. The idea is that individual fermions moving with Fermi velocity v_F hit the wall with mean time $\sim R/v_F$; the inverse time $\sim v_F/R$ then determines the contribution to the width arising from wall effects—both for $\Delta\Gamma$ and $\Gamma^{\uparrow}$. The subject of one-body dissipation has also been discussed extensively in the nuclear physics literature [27–29]. The width $\Gamma^{\downarrow}$, on the other hand, arises from two-particle collisions. We expect $\Gamma^{\downarrow}$ to vary smoothly with energy and nuclear size for magic cases, since the collisional mean free path λ shows similar smooth variations [30]. The average time between two collisions is $\sim \lambda/v_F$ and hence $\Gamma^{\downarrow}$ is expected to be $\sim v_F/\lambda$. This is the only contribution in the $R \to \infty$ limit.

The total intrinsic width is thus expected to be

$$\Gamma_i = \Gamma^{\downarrow}_{\infty} + c\hbar v_F/R, \tag{4}$$

where $\Gamma^{\downarrow}_{\infty}$ is the spreading width in the bulk limit, and c is a constant. This is in agreement with (2) and the data presented in figure 2 for spherical, magic nuclei.

It is interesting to consider the limit $R \to \infty$, corresponding to nuclear matter or the bulk metal. From figure 2, we see that if the straight lines are extrapolated towards $(k_F\tilde{R})^{-1} = 0$, the resulting intercept on the Γ/ε_F axis is much larger for nuclei than for metal particles. This is not too surprising, as $k_F\lambda$ is much smaller in nuclear-matter [30] than in bulk metals at room temperature [20], reflecting the greater effect of collisions in the former case. The limiting contribution $\Gamma^{\downarrow}_{\infty}$ constitutes a substantial fraction of the total width for spherical nuclei; for ^{208}Pb it is about 50% [31]. On the other hand, for metal particles of comparable A, the contribution $\Gamma^{\downarrow}_{\infty}$ constitutes a much smaller fraction of Γ_i.

3.3 *Resonance widths: shell effects*

So far we have discussed only the monotonic variation of the FWHM that obtains for spherical nuclei. As we see from figure 1, when we consider *all* nuclei, superimposed on this monotonic variation, there are striking and strong shell-structure linked oscillations in the FWHM. (As mentioned in § 2.2, the FWHM in metal clusters also seems to show similar tendencies.) We discuss the origin of these oscillations in two broad representative regions, namely $150 < A < 190$ and $80 < A < 150$.

In the range $150 < A < 190$, Dietrich and Berman [9] have fitted two-component Lorentz curves to the photoneutron cross section data. This indicates a splitting of the line, due to deformation of the nucleus. As in § 2·1, we denote the two resonance energies by ω_{01} and ω_{02}, with $\omega_{01} < \omega_{02}$, and the corresponding widths by Γ_1 and Γ_2. For a spheroidal deformation, (1) leads us to expect that ω_{01} and ω_{02} correspond to oscillations along the semimajor and semiminor axes respectively. Equation (4) then implies that $\Gamma_1 < \Gamma_2$. This is indeed found to be true, for $150 < A < 190$, for the values of the widths tabulated by Dietrich and Berman [9]. In fact, with the exceptions of ^{55}Mn and ^{63}Cu, this is true for all the nuclei listed there. This provides additional evidence for the overall decrease of the intrinsic width with increasing radius. The corresponding cross sections σ_1 and σ_2 also generally satisfy $\sigma_1 < \sigma_2$. The increase of the FWHM away from the spherical cases can be ascribed, at least partially, to the fact that deformations produce a splitting of the line, and also cause $\Gamma_2 > \Gamma (> \Gamma_1)$, where Γ would be the width if the nucleus were undeformed. Since deformations of the shape follow shell-structure systematics, with smallest deformations close to the magic numbers, so does the FWHM [32].

In the region $80 < A < 150$, Dietrich and Berman [9] have fitted one-component Lorentz curves to the photoneutron cross section data (with the exceptions of ^{127}I and ^{148}Nd). As is clear from figure 1, oscillations of the FWHM versus A in this region are as prominent as those for $150 < A < 190$. Thus, even when the line is unsplit, the width of the best-fit Lorentzian oscillates as a function of A, with minima at the magic numbers. This indicates that the intrinsic width Γ_i can itself show shell-structure linked oscillations. [33] Bergère [10] has correlated the FWHM in this region with the ratio $E(4^+)/E(2^+)$, which characterizes the 'softness' of nuclei. Here $E(J^+)$ is the energy of the first J^+ state in the nuclear spectrum.

The theoretical considerations we have presented in this section are schematic, and aimed at understanding the empirical systematics observed—in contrast to more detailed theoretical studies of the width for *individual* nuclei.

4. Conclusion

We conclude by recapitulating the main points of this paper. The FWHM of the total photoneutron cross section shows shell-structure-linked oscillations as a function of A even for $3 < A < 50$. Disregarding oscillations, for instance by focusing on magic nuclei, the FWHM generally decreases with increasing A approximately as $A^{-1/3}$ (see (4)). Striking similarities are seen when the FWHMs for nuclei are compared with photoabsorption FWHMs in small metal particles, after proper rescaling of the energies and lengths.

The systematics which have been pointed out and discussed in this paper bring the task of a theory into better focus. While a complete theory has not been presented here, we have given a schematic theoretical description which allows one to understand

at least the principal trends. However, it is the empirical observations which constitute the main result of this paper.

Acknowledgements

We are grateful to C V K Baba, R K Bhaduri, V Subrahmanyam and C S Warke for very useful discussions and comments on the manuscript, and to B L Berman for bringing the work of Dietrich and Berman [9] to our attention. A part of the work was done when RSB was visiting McMaster University, Hamilton, Canada, and a part when MB was visiting the Department of Theoretical Physics, University of Oxford, UK. The hospitality of both institutions is gratefully acknowledged.

References

[1] S Sugano, in *Microclusters* edited by S Sugano, Y Nishina and S Ohnishi (Springer Berlin, 1987)
[2] W A de Heer, W D Knight, M Y Chou and M L Cohen, *Solid state physics* **40**, 93 (1987)
[3] B L Berman and S C Fultz, *Rev. Mod. Phys.* **47**, 713 (1975)
[4] A van der Woude, *Prog. Part. Nucl. Phys.* **18**, 217 (1987)
[5] M Born and E Wolf, *Principles of optics* (Pergamon, Oxford, 1970) ch. 13
[6] S P Apell, J Giraldo and S Lundqvist, *Phase Transitions* **24–26**, 577 (1990)
[7] V V Kresin, *Phys. Rep.* **220**, 1 (1992)
[8] M Barma and R S Bhalerao, in *Physics and chemistry of finite systems: from clusters to crystals* edited by P Jena, S N Khanna and B K Rao (Kluwer, Dordrecht, 1992) NATO ASI Sr. **Vol II**, p. 881
[9] S S Dietrich and B L Berman, *At. Data Nucl. Data Tables* **38**, 199 (1988)
[10] R Bergère, in *Photonuclear reactions* edited by S Costa and C Schaerf, Lecture Notes in Physics (Springer, Berlin, 1977) **61**, 114
[11] K A Snover, *Ann. Rev. Nucl. Part. Sci.* **36**, 545 (1986)
[12] Although ^{28}Si is not a magic nucleus, it displays behaviour similar to a magic nucleus in at least one other context: the plot of nuclear electric quadrupole moment vs Z or N passes through a zero near ^{28}Si, indicating a prolate to oblate transition. Similar transitions also occur at the magic numbers [13].
[13] M A Preston and R K Bhaduri, *Structure of the nucleus* (Addison–Wesley, Reading, 1975) figs. 3.2 and 10.12 pages 73 and 470
[14] U Kreibig and L Genzel, *Surf. Sci.* **156**, 678 (1985)
[15] K Selby, M Vollmer, J Masui, W A de Heer and W D Knight, *Phys. Rev.* **B40**, 5417 (1989)
[16] K Selby, V Kresin, J Masui, M Vollmer, A Scheidemann and W D Knight, *Z. Phys.* **D19**, 43 (1991)
[17] J Tiggesbäumker, L Köller, H O Lutz and K H Meiwes-Broer, *Chem. Phys. Lett.* **190**, 42
[18] W D Myers, W J Swiatecki, T Kodama, L J El-Jaick and E R Hilf, *Phys. Rev.* **C15**, 2032 (1977)
[19] K P Charlé, W Schulze and B Winter *Z. Phys.* **D12**, 471 (1989)
[20] N W Ashcroft and N D Mermin, *Solid state physics* (Holt, Rinehart and Winston, New York, 1976) ch. 1
[21] M Goldhaber and E Teller, *Phys. Rev.* **74**, 1046 (1948)
[22] H Steinwedel and J H D Jensen, *Z. Naturforschung* **5a**, 413 (1950)
[23] U Kreibig, *J. Phys.* **F4**, 999 (1974)
[24] A Kawabata and R Kubo, *J. Phys. Soc. Jpn.* **21**, 1765 (1966)
[25] M Barma and V Subrahmanyam, *J. Phys. Cond. Matter* **1**, 7681 (1989)
[26] C Yannouleas and R Broglia, *Ann. Phys. (NY)* **217**, 105 (1992)
[27] D M Brink, *Nucl. Phys.* **4**, 215 (1957)
[28] J Blocki, Y Boneh, J R Nix, J Randrup, M Robel, A J Sierk and W J Swiatecki, *Ann. Phys. (NY)* **113**, 330 (1978)

[29] C Yannouleas, *Nucl. Phys.* **A439**, 336 (1985)
[30] J Wambach, *Rep. Prog. Phys.* **51**, 989 (1988)
[31] For real nuclei, the full two-body contribution $\Gamma^{\downarrow}$ may differ significantly from $\Gamma^{\downarrow}_{\infty}$.
[32] K Okamoto, *Phys. Rev.* **110**, 143 (1958)
[33] This is in contrast to the statements made in various reviews [34–37] that the width, like ω_0, varies smoothly with A.
[34] J Speth and A van der Woude, *Rep. Prog. Phys.* **44**, 719 (1981)
[35] K Goeke and J Speth, *Ann. Rev. Nucl. Part. Sci.* **32**, 65 (1982)
[36] M N Harakesh, contribution to *XVII Summer School on nuclear structure by means of nuclear reactions*, Mikolajki, Polland 1985 (unpublished)
[37] A van der Woude, in *electric and magnetic giant resonances in nuclei* edited by J Speth (World Scientific, Singapore, 1991) 100